

# Advantages of long-axis PROPELLER EPI via $k$ -space weighting: comparison of point spread function with short-axis PROPELLER EPI

T-C. Chuang<sup>1</sup>, T-Y. Huang<sup>2</sup>, F-N. Wang<sup>3</sup>, and H-W. Chung<sup>1</sup>

<sup>1</sup>Electrical Engineering, National Taiwan University, Taipei, Taiwan, <sup>2</sup>Electrical Engineering, National Taiwan University of Science and Technology, Taipei, Taiwan, <sup>3</sup>Biomedical Engineering and Environmental Sciences, National Tsing Hua University, Hsinchu, Taiwan

## Introduction

PROPELLER EPI has been introduced [1] to substantially decrease the susceptibility-related geometric distortion along phase-encoding direction in single-shot EPI, which is severer at high fields. However, artifacts due to strong field inhomogeneities may still appear in the form of image blurring. Recently, another type of PROPELLER EPI technique [2] using the short side, rather than the traditionally long side, of blades as EPI readout direction was proposed to show that the blurring effect can be dramatically reduced due to largely shortened echo spacing. Nevertheless, the results shown in [2] did not consider the  $k$ -space weighting scheme which has been used for de-blurring [1, 3] by emphasizing the contribution of data near the spin-echo where less off-resonance phase error was accumulated. In this simulation study, we demonstrated that long-axis PROPELLER (LAP) EPI and short-axis PROPELLER (SAP) EPI can benefit differently from the weighting window due to distinct sampling trajectories.

## Materials and Methods

The  $k$ -space weighting scheme was performed only for data points acquired by multiple blades in the process of PROPELLER reconstruction after phase correction, spatial registration, and regridding were done. Here a windowing function exponentially decaying from the center [3] was applied along the phase-encoding direction as  $w(n) = \exp(-\lambda \cdot n)$ , where  $n$  indicates the number of  $k$ -lines away from the center line in each blade. A larger  $\lambda$  tends to rely much more on the data at fewer phase-encoding steps, which were less prone to the off-resonance errors. Note that constant weighting was applied along readout direction due to rapid sampling. Examples of the  $k$ -space weighting schemes ( $\lambda = 0.1$ ) were demonstrated in Fig. 1a (LAP-EPI) and Fig. 1b (SAP-EPI).

To investigate the reduction of blurring that can be brought by the  $k$ -space weighting scheme, point spread functions (PSF) of LAP-EPI and SAP-EPI were simulated under constant off-resonance frequency ( $\gamma\Delta B_0$ ) of 10~40 Hz over the entire field of view (FOV). Twenty-six blades in size of 256(readout) $\times$ 32(phase) and 32 $\times$ 256 were generated respectively to mimic raw data of LAP-EPI and SAP-EPI. A  $T2^*$  of 40 ms was considered while  $T2$  relaxation was neglected. The echo spacing of 1 ms and 0.25 ms (i.e. constant readout bandwidth), resulting in a spatial displacement of 3% and 0.75% FOV along phase-encoding in single-shot EPI, were set for 256 and 32 readout lengths according to routine parameters on clinical scanners. Zero-padding was performed on the  $k$ -space to achieve 10 times resolution in image domain. In addition to PSF, Shepp-Logan phantom was also sampled in the same way and reconstructed by different weighting schemes ( $\lambda = 0$  and 0.5) to demonstrate the reduction of image blurring.

## Results

Figure 2a compared the enlarged cross-sectional views of normalized PSF of LAP-EPI using four  $k$ -space weighting schemes ( $\lambda = 0, 0.1, 0.2,$  and  $0.5$ ) at 30 Hz off-resonance. It can be easily observed that a larger  $\lambda$ , which places less weighting on the  $k$ -lines far away from center, significantly lowers the magnitude of side lobes. Therefore, the strong image blurring in the Shepp-Logan phantom reconstructed with the uniform weighting (Fig. 2b), i.e.,  $\lambda = 0$ , was largely eliminated in Fig. 2c when  $\lambda = 0.5$ . However, little difference was found between PSFs of SAP-EPI with different weighting functions (Fig. 3a) at 30 Hz off-resonance. The image quality of SAP-EPI in Figs. 3b ( $\lambda = 0$ ) and 3c ( $\lambda = 0.5$ ) was visually similar and both had less blurring than Fig. 2a. However, Fig. 2c, the LAP-EPI image reconstructed with a sharper weighting function, exhibits even better sharpness in close similarity to the original Shepp-Logan phantom than the SAP-EPIs shown in Figs. 3b and 3c. Similar phenomena were found in PSF at different off-resonance fields (not shown).

## Discussion

Results in this study revealed that the  $k$ -space weighting scheme dramatically improved sharpness on LAP-EPI. Little influence was found for SAP-EPI, where data suffering less from off-resonance distribute densely in the central  $k$ -space with its sampling trajectory [2]. For any grid point covered by multiple blades, SAP-EPI combines data contributed by different shots carrying comparable off-resonance errors, making the  $k$ -space weighting always close to a simple arithmetic averaging. In LAP-EPI, data of good quality spread over entire the  $k$ -space and become dominant during the combination of blades through the use of the  $k$ -space weighting scheme. As a result, LAP-EPI using a proper weighting function has potentials to obtain images without blurring (Fig. 2c) at the cost of SNR [3]. These important properties can be utilized for further optimization of image quality in PROPELLER-EPI.

**References:** 1. Wang FN et al., MRM 2005;54:1232-1240. 2. Skare S, et al. MRM 2006;55:1298-1307.



**Fig.1**  $k$ -space weighting schemes for single blade of LAP-EPI (a) and SAP-EPI (b) at a  $\lambda$  of 0.1. Note that the phase encoding direction is vertical in a and horizontal in b.

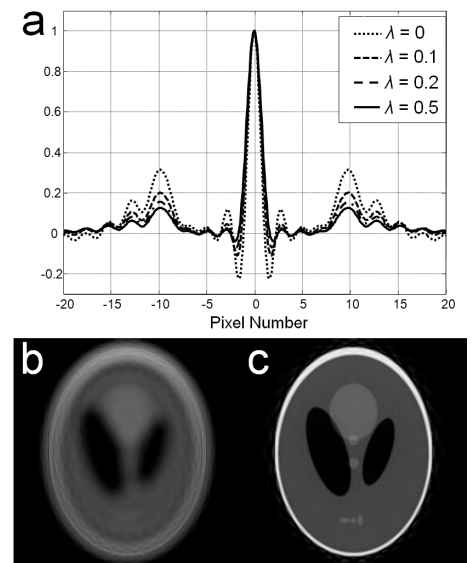


**Fig.2a** PSF profiles of LAP-EPI with different  $k$ -space weighting schemes ( $\lambda = 0, 0.1, 0.2,$  and  $0.5$ ). **b** and **c** were Shepp-Logan phantom images reconstructed by the same set of data at  $\lambda$  of 0 and 0.5 respectively.

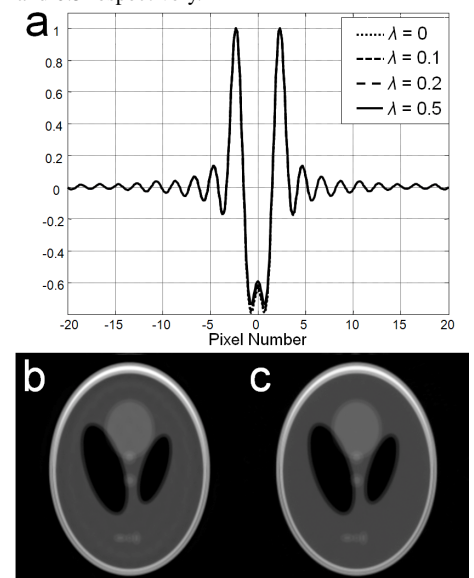


**Fig.3a** Simulation results of SAP-EPI in the same way as in Fig.2. Shepp-Logan phantom images reconstructed with different functions were shown in **b** ( $\lambda=0$ ) and **c** ( $\lambda=0.5$ ).

3. Chuang TC et al., ISMRM 2006; abst no. 2955.